



This is a repository copy of *Multimodal super-resolution optical microscopy using a transition metal-based probe provides unprecedented capabilities for imaging both nuclear chromatin and mitochondria.*

White Rose Research Online URL for this paper:

<https://eprints.whiterose.ac.uk/122534/>

Version: Accepted Version

---

**Article:**

Sreedharan, S., Gill, M., Garcia, E. et al. (9 more authors) (2017) Multimodal super-resolution optical microscopy using a transition metal-based probe provides unprecedented capabilities for imaging both nuclear chromatin and mitochondria. *Journal of the American Chemical Society*, 139 (44). pp. 15907-15913. ISSN 0002-7863

<https://doi.org/10.1021/jacs.7b08772>

---

**Reuse**

Items deposited in White Rose Research Online are protected by copyright, with all rights reserved unless indicated otherwise. They may be downloaded and/or printed for private study, or other acts as permitted by national copyright laws. The publisher or other rights holders may allow further reproduction and re-use of the full text version. This is indicated by the licence information on the White Rose Research Online record for the item.

**Takedown**

If you consider content in White Rose Research Online to be in breach of UK law, please notify us by emailing [eprints@whiterose.ac.uk](mailto:eprints@whiterose.ac.uk) including the URL of the record and the reason for the withdrawal request.



[eprints@whiterose.ac.uk](mailto:eprints@whiterose.ac.uk)  
<https://eprints.whiterose.ac.uk/>

# Multimodal super-resolution optical microscopy using a transition metal-based probe provides unprecedented capabilities for imaging both nuclear chromatin and mitochondria.

Sreejesh Sreedharan<sup>1</sup>, Martin R Gill<sup>2,3</sup>, Esther Garcia<sup>4</sup>, Hiwa K Saeed<sup>1</sup>, Darren Robinson<sup>2</sup>, Aisling Byrne<sup>6</sup>, Ashley Cadby<sup>5</sup>, Tia E. Keyes<sup>6</sup>, Carl Smythe<sup>2</sup>, Patrina Pellett\*<sup>6</sup>, Jorge Bernardino de la Serna\*<sup>4,8</sup>, and Jim. A. Thomas\*<sup>1</sup>.

<sup>1</sup> Department of Chemistry, University of Sheffield, Sheffield, UK

<sup>2</sup> Department of Biomedical Science, University of Sheffield, Sheffield, UK

<sup>3</sup> Current address: CRUK/MRC Oxford Institute for Radiation Oncology, Department of Oncology, University of Oxford, Oxford, UK

<sup>4</sup> Central Laser Facility, Science and Technology Facilities Council, Rutherford Appleton Laboratory, Research Complex at Harwell, Harwell-Oxford, UK

<sup>5</sup> The Department of Physics and Astronomy, University of Sheffield, Sheffield, UK

<sup>6</sup> School of Chemical Sciences, National Centre for Sensor Research, Dublin City University, Dublin 9, Ireland

<sup>7</sup> GE Healthcare Bio-Sciences Corp, 800 Centennial Avenue, P.O. Box 1327, Piscataway, NJ 08855-1327 USA

<sup>8</sup> Department of Physics, King's College London, London, UK.

**KEYWORDS** (*Word Style "BG\_Keywords"*). If you are submitting your paper to a journal that requires keywords, provide significant keywords to aid the reader in literature retrieval.

---

**ABSTRACT** Detailed studies on the live cell uptake properties of a dinuclear membrane permeable Ru<sup>II</sup> cell probe show that, at low concentrations, the complex localizes and images mitochondria. At concentrations above ~20  $\mu$ M the complex images nuclear DNA. Since the complex is extremely photostable, has a large Stokes shift, and displays intrinsic subcellular targeting, its compatibility with super-resolution techniques was investigated. It was found to be very well suited to image mitochondria and nuclear chromatin in two colour, 2C-SIM; and STED and 3D-STED, both in fixed and live cell. In particular, due to its vastly improved photostability compared to conventional SR probes, it can provide images of nuclear DNA at unprecedented resolution.

---

## Introduction

Techniques such as fluorescence-based confocal laser scanning microscopy (CLSM) have led to the development of organelle specific emissive probes, facilitating real-time live cell imaging of cellular processes and the possibility of optical sectioning.<sup>1-6</sup> Yet, there are still drawbacks to these methods. Due to the relationship between resolution and the wavelength of imaging light, first defined by Abbé, the practical limit of optical microscopy is restricted to features above ~250 nm.<sup>7</sup> Solutions to the drawback of the Abbé limit have emerged, through the development of super-resolution microscopy (SRM).<sup>3,8-10</sup>

Two of the most employed approaches to SRM, stimulated emission depletion (STED) microscopy<sup>11,12</sup> and structured illumination microscopy (SIM),<sup>13</sup> provide contrasting features. In STED, selective deactivation of photo-excited dye molecules through a depletion beam provides outstanding spatial resolution but requires luminophores with exacting photoexcitation properties and/or photostability.<sup>14,15</sup> Furthermore, in live cell work, multiple image acquisition cycles can lead to poor temporal resolution and also expose probes

and cells to potentially deleterious total light exposures many magnitudes higher than conventional conditions.

By contrast, although SIM provides appreciably lower resolution limits (~140 nm) it requires much lower acquisition times and considerably less light exposure, meaning that this technique is eminently suited to live cell imaging and 3-D sectioning.<sup>13,16</sup>

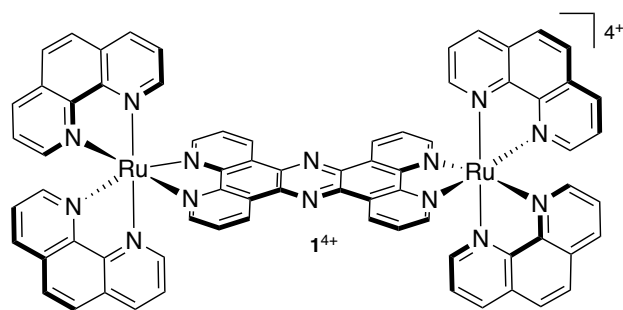
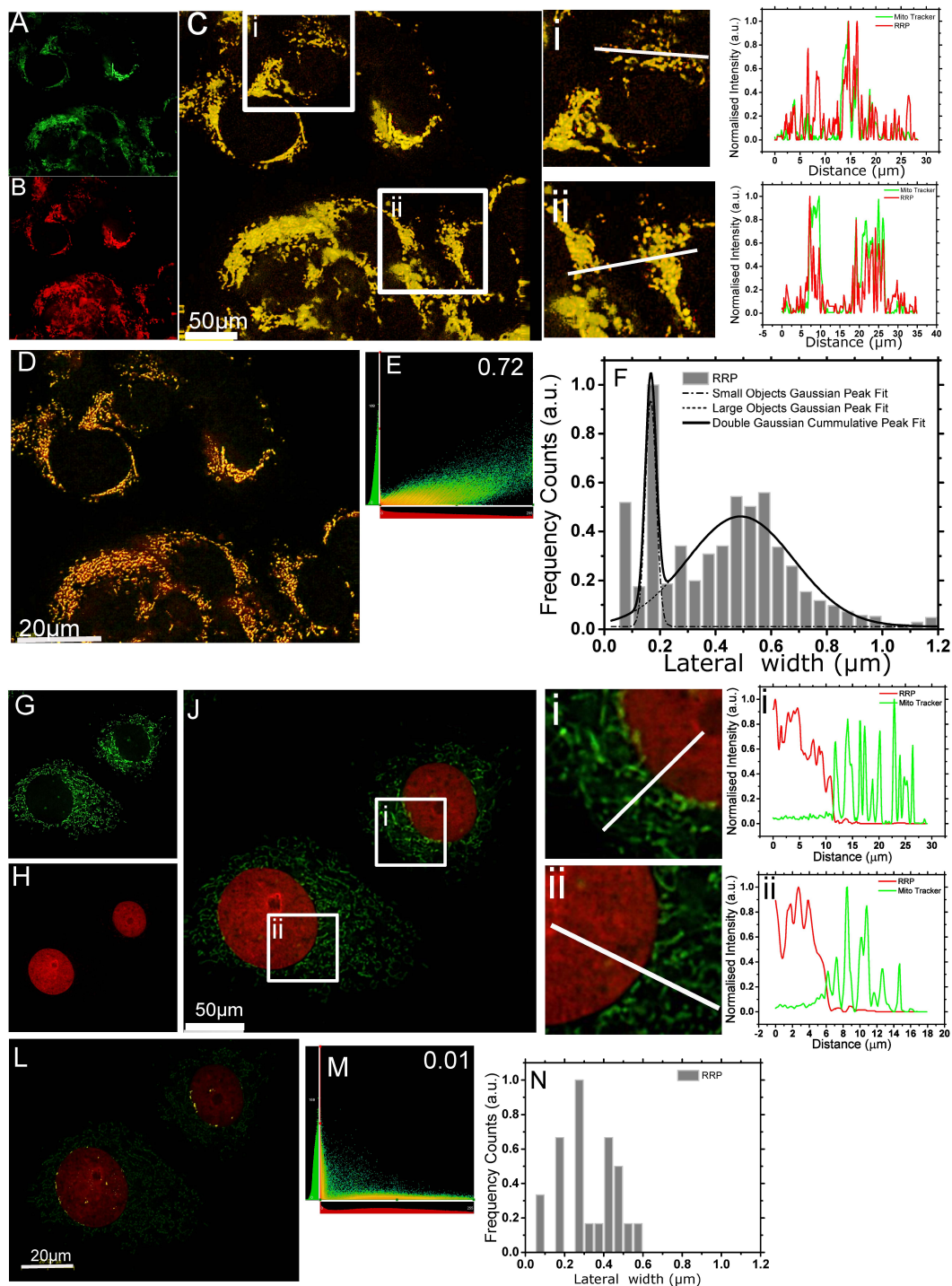


Figure 1. Structure of complex **1<sup>4+</sup>** studied in this report



**Figure 2:** Representative wide field deconvolved images of MCF7 cells stained with MTR (green) and co-stained with  $[1]Cl_4$  (red) at two different concentrations. Images A – F: staining at  $4 \mu M$  showing separate MTR (A) and  $[1]Cl_4$  (B) signals; combined images of MTR and  $[1]Cl_4$  signals (C); colocalization maps, displaying only the colocalized objects (D) and calculated Pearson's coefficients (E); population distribution analysis of lateral width (F), obtained from the colocalization map in D. Images G – L: equivalent data for staining at  $18 \mu M$ . In both cases images (i, ii) are zoomed-in details from the insets with intensity profiles shown (right); population distribution analysis of lateral width (N), obtained from the colocalization map in L. The structures resolved at  $4 \mu M$  could be fitted to a double Gaussian distribution while the structures at  $18 \mu M$  of  $[1]Cl_4$  could not, indicating a population of colocalizing objects with two different widths.

In recent years, the use of transition metal complexes as imaging agents for specific biomolecules and structures have been explored as they have many potential advantages over conventional probes.<sup>17-21</sup> A case in point has been the live cell microscopy probe based on a dinuclear  $Ru^{II}$ -based complex  $1^{4+}$ , Fig. 1, which does not emit in aqueous solution

until it is bound to DNA or a lipophilic membrane, thus reducing signal to noise in imaging such structures.<sup>22,23</sup>

This complex has multifunctional imaging modalities. Since it also displays emission at near infrared wavelengths minimizing its phototoxicity  $1^{4+}$  it is well suited to CLSM,

imaging the structure of nuclear DNA within fixed and live cell nuclei.<sup>24</sup> Thanks to its long lifetime when bound to DNA, it is also a probe for the lifetime imaging microscopy<sup>25</sup>. Finally, its use is not restricted to optical techniques as - along with its Os<sup>II</sup> derivative<sup>24,26</sup> - it is a convenient, easy to handle, contrast agent for transmission electron microscopy, TEM. Given all these facts it struck us that complex **1**<sup>4+</sup> had excellent potential as a SR probe; particularly as recent studies by the Keyes group have demonstrated that Ru<sup>II</sup> complexes tagged to cell penetrating peptide moieties are nuclear STED probes.<sup>27</sup> Since, SIM and STED offer contrasting advantages,<sup>28</sup> we investigated the application of **1**<sup>4+</sup> for each technique and have found that it is well suited to both. These studies also reveal that since the subcellular localisation of the complex is concentration dependent it can be used to image both mitochondria and DNA through either technique. In particular, due to a unique combination of binding selectivity and extreme photostability, it produces 3-D STED images of nuclear DNA at unprecedented resolution.

## Results and Discussion

Although the live cell uptake of **1**<sup>4+</sup> was originally investigated through CLSM at high concentrations,<sup>24</sup> studies to determine the minimum concentration of **1**<sup>4+</sup> required to obtain clear nuclear uptake and visualization were carried out using conventional wide field microscopy. These experiments involved exposing MCF7 breast cancer cell line to a range of probe concentrations from 250 nM upward, showed that rapid nuclear localization occurs even at low concentrations; for example, bright staining is observed within two minutes of exposure at 10  $\mu$ M concentration - see SI.

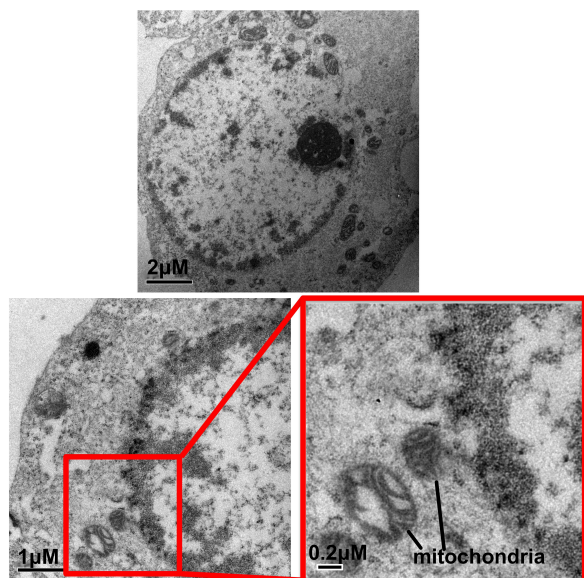


**Figure 3.** TEM micrographs using [1]Cl<sub>4</sub> by MCF-7 cells (treatment: 500  $\mu$ M, 1 h) as the sole contrast agent. Progressively magnified images clearly reveal localization within mitochondria.

Interestingly, at lower concentrations, emissive signals were observed from the cytosol region. Since lipophilic cations - in which charge is distributed over large hydrophobic surface areas - often accumulate in mitochondria<sup>29</sup>, the possibility that **1**<sup>4+</sup> localizes in these organelles at lower concen-

trations was investigated. Co-staining was carried out using Mito Tracker Red, MTR, which displays an emission that is close to that of **1**<sup>4+</sup>, but an excitation wavelength that is well separated from the complex, allowing both probes to be addressed separately.

A detailed colocalization analysis was carried out at probe concentrations of 4  $\mu$ M and 18  $\mu$ M. Examples of the collected images and quantification, shown in Fig. 2, illustrate that strong co-localization between **1**<sup>4+</sup> and MTR is observed at concentrations below 5  $\mu$ M, but dye overlap analyses clearly indicate that with increasing concentrations of **1**<sup>4+</sup> the metal complex starts to localize in the nucleus too. At concentrations above 18  $\mu$ M, mitochondrial emission from the probe is not discerned due to its more intense emission when bound to DNA. The possibility, that **1**<sup>4+</sup> exclusively localises in the nucleus through a transport mechanism functioning at higher probe concentrations was discounted through parallel TEM studies. At concentrations used to obtain the bright nuclear staining of live cells in CLSM (500  $\mu$ M), TEM images revealed that **1**<sup>4+</sup> is still localized within mitochondria. At highest magnifications it is apparent that the complex is located in the inter-membrane space, not the central lumen where mtDNA is located - Figure 3. Although previous studies have shown that **1**<sup>4+</sup> displays low cytotoxicity, more detailed experiments also confirm that the complex does not disrupt mitochondrial membrane potentials - See SI.

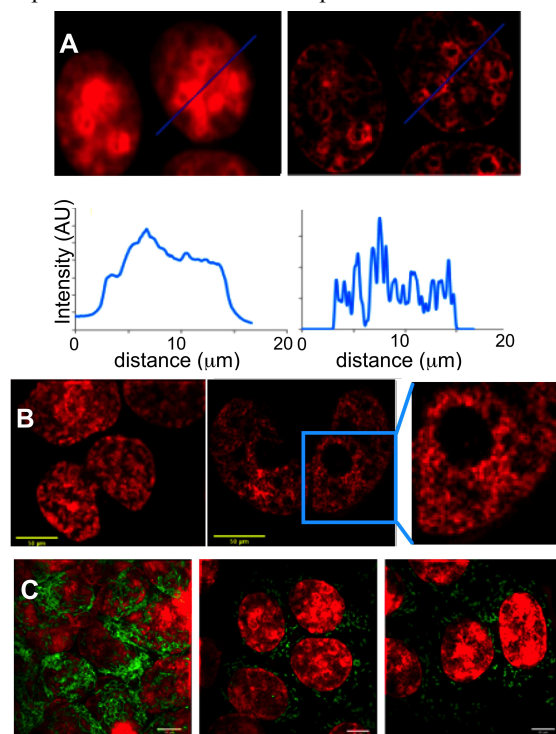


**Figure 4:** (A) Top: a comparison of wide-field microscope (left) and SIM image (right) produced by staining A2780 cells with [1]Cl<sub>4</sub> at concentration = 25  $\mu$ M. Bottom: Emission intensity maps along blue line of the images, showing enhanced resolution in SIM. (B) Single colour SIM imaging of chromatin within nuclei of A2780 cells using [1]Cl<sub>4</sub> (concentration = 50  $\mu$ M). (C) Dual colour SIM imaging of MCF7 cells using [1]Cl<sub>4</sub> at concentration = 25  $\mu$ M and the mitochondrial stain, MTR (1  $\mu$ M). Pseudo color has been employed in all the images, Scale bar: 10  $\mu$ m.

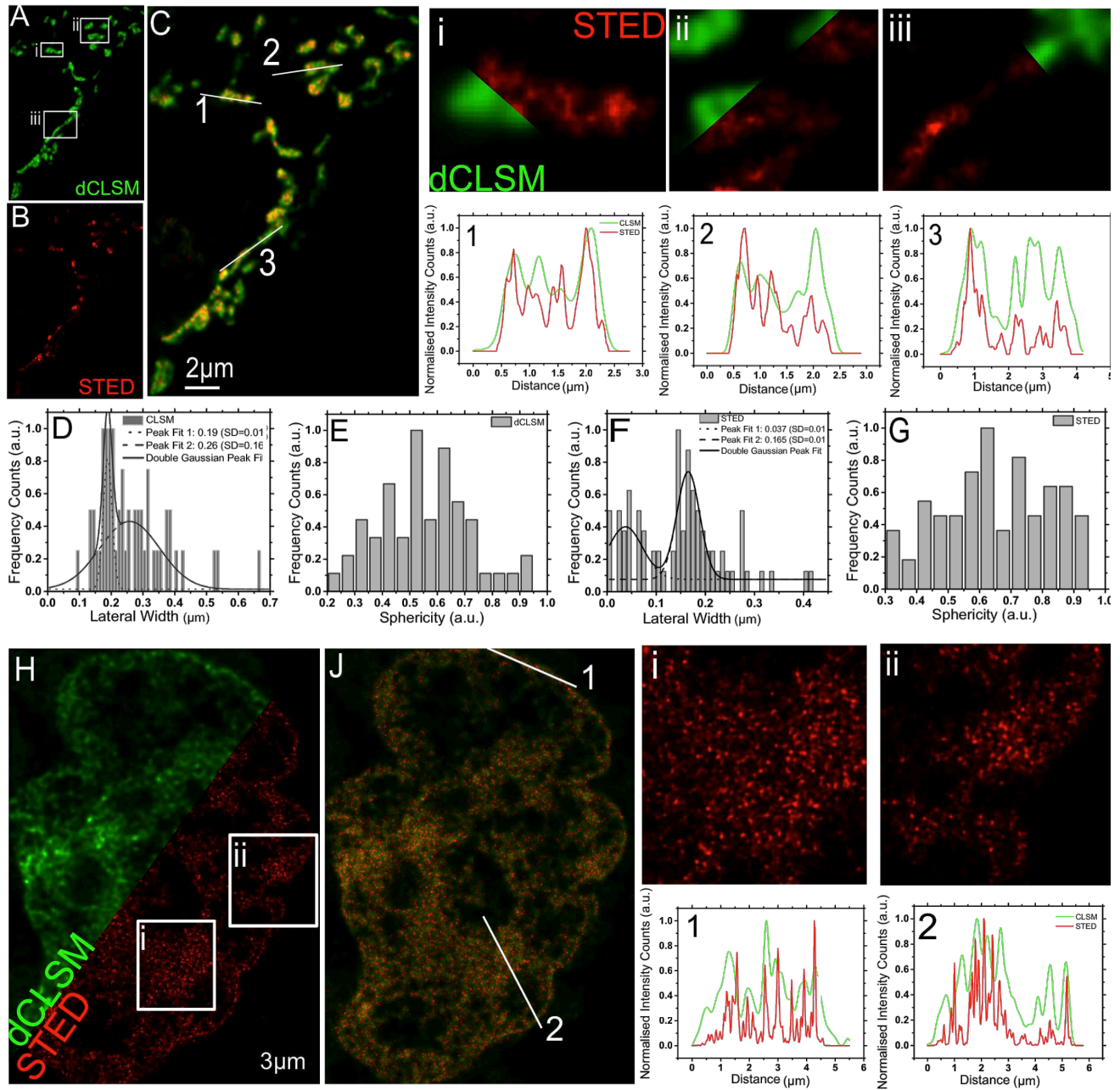


**Figure 5:** Super resolution STED microscopy of [1]Cl<sub>4</sub> stained MCF-7 compared to deconvoluted CLSM using a HyVision, employing 0.5 airy units pinhole aperture. Images **A - G**: Mitochondria staining at 6 μM [1]Cl<sub>4</sub>, HyVision images shown in green deconvolved (**A**) STED image in red (**B**), merged image is shown in (**C**). White squared insets in **A**, are magnified in (**i**, **ii**, **iii**) Enhancement of the resolution by STED can be observed in the compared-merged dCLSM/STED images. Quantification of the resolved imaged by dCLSM and STED is shown in (**D - G**), Gaussian peak fits of the population distribution of the lateral width (**D**, **F**) and sphericity (**E**, **G**) of mitochondria. Mitochondria revealed by STED were smaller than 50 nm in width, STED also revealed more a distribution of sphericity displaced towards higher values. Intensity profile diagrams of the lines drawn in **C** showing STED resolution improvement are shown in **1**, **2**, **3**. Lines in red and green show STED and dCLSM respectively. Images **H**, STED and HyVision comparison images of nucleus stained by [1]Cl<sub>4</sub> and the merged image (**J**), white squared insets are magnified in (**i**, **ii**) and the comparative STED and HyVision intensity profile for the white lines drawn in **J** are shown in (**1**, **2**)

Taken together, the optical microscopy and TEM studies demonstrate that, at low concentrations, complex 1<sup>4+</sup> localizes in mitochondria, but at higher concentrations - when binding to this intracellular target is saturated - the probe also binds to nuclear DNA. A similar concentration dependent uptake profile is observed for the natural product berberine,<sup>30</sup> high-resolution CLSM-based Airyscan microscopy also supports these findings – See ESI.

Having established that 1<sup>4+</sup> is a concentration-dependent probe for both mitochondria and nuclear DNA using conventional optical microscopy, its use as a SR probe was initially explored using SIM. Unfortunately, at the low concentrations required to obtain mitochondrial localization, the emission from 1<sup>4+</sup> is not bright enough to obtain high quality images. However, striking results are obtained when 1<sup>4+</sup> is used at concentrations above 20 μM.

The low photobleaching and bright nucleus localised emission of  $\mathbf{1}^{4+}$  is ideally suited to SIM imaging, particularly as images could be collected using the existing Alexa Fluor 647 channel of the Delta Vision OMX-SIM system, revealing details of chromatin structure illustrated by the images and intensity maps in Fig. 4A and B. To dissect the dynamics of cellular processes, simultaneous imaging of separate organelles and other cell structures at sub-diffraction resolution is often required; this goal can be accomplished by two-colour SR microscopy<sup>31</sup>. Therefore, we also explored the use of  $\mathbf{1}^{4+}$  as a co-stain in 2C-SIM. The spectral properties of the complex suggested that it is well suited for use with a range of commercial probes; to establish its potential in this context we investigated the Mito Tracker series. Several members of the series such as Mito Tracker Green proved to be insufficiently stable for SIM as - when exposed to the light and acquisition cycle required for imaging, considerable photobleaching occurred - see SI. Indeed, in our hands, Mito Tracker Red, MTR, was the only member of this series that was compatible with the demands of SIM conditions. However, the combination of  $\mathbf{1}^{4+}$  at concentrations above 18  $\mu\text{M}$  and MTR resulted in minimum co-localization, producing detailed 2C-SIM images of both chromatin and mitochondria in MCF7 cells - Fig 4C.

The high quality of the SIM images over extended collection periods confirmed the photostability of the dye. Since emission from the bound complex is long lived (180 ns) which increases the probability of stimulated emission and it displays a large Stoke Shift - which minimizes self-quenching even at high dye loading and provides “spectral width” for emission, excitation, and depletion<sup>32</sup> - the use of  $\mathbf{1}^{4+}$  as a STED probe was then investigated. Initial studies, carried out using conditions reported for Ru(II) peptide conjugates<sup>27</sup> - in which a 660 nm depletion beam was used - proved to be unsuccessful. Such observations usually indicate photoexcitation into a dark state. To address this issue, depletion using a 775 nm beam into the low energy edge of the probe’s broad emission was carried out. In this second set of conditions, STED images were successfully obtained and - using concentrations of  $\mathbf{1}^{4+}$  as low as 6  $\mu\text{M}$  - SR imaging of mitochondria could now be accomplished - Fig 5 A-G. Satisfyingly - and consistent with the wide field and SIM studies - at higher treatment concentrations the probe produced striking images of chromatin DNA with the improved resolution clearly shown in comparative Intensity profile diagram - Figure 5 H and J.

Thanks to the low phototoxicity of the dye we also found that it was suited to use in live-cell STED imaging. Using concentrations used in our previous CLSM studies on live cell imaging we obtained excellent quality images, such as those show in Fig. 6.

While conventional STED provides high-resolution in two-dimensions, resolving the relative spatial arrangements of complex subcellular structures in three-dimensions is vital in fully determining morphologies and often provides fundamental insights into biological function. This need has led to the development and implementation of 3D-STED,<sup>33,34</sup> however successful implementation of this technology requires highly photo-stable luminophores<sup>35</sup> as the optical sectioning procedures used to generate 3D-STED images require a probe that can withstand prolonged exposure to

optically demanding conditions which often lead to photobleaching of conventional probes

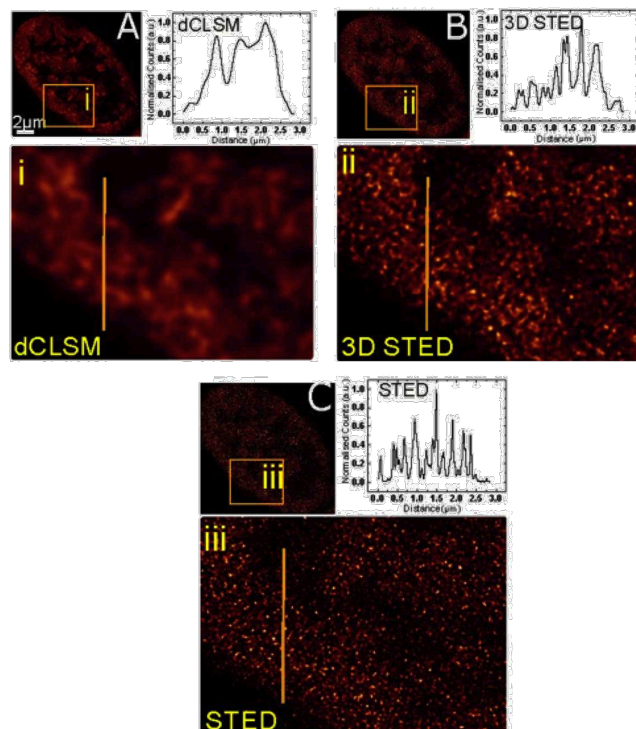


**Figure 6:** Images of live-cell staining by 500  $\mu\text{M}$   $[\mathbf{1}]_{\text{Cl}_4}$ : HyVolution (dCLSM) (A), 3D STED (B) and STED (C); Magnified insets (i-iii) and fluorescence intensity profiles from i-iii is shown inset.

Since the most notable feature of  $\mathbf{1}^{4+}$  in terms of its optical properties is its extreme stability under prolonged laser illumination its use in 3-D STED was also investigated. Gratifyingly, thanks to its superlative photostability and minimal photobleaching, probe  $\mathbf{1}^{4+}$  use as a STED luminophore facilitated the generation of 3D-images of nuclear chromatin (requiring laser exposures of up to an hour) with excellent resolution in all three planes (XY resolutions  $\approx$  35 nm and 150nm in the Z-axis) as illustrated by the images shown in Fig 7.

## Conclusions

Membrane permeable complex  $\mathbf{1}^{4+}$ , which can be used to image mitochondria and the nucleus through optical microscopy - is a probe for both SIM and STED. SIM images of chromatin are obtained at probe concentrations above 25  $\mu\text{M}$  and it can be used for 2C-SIM with a commercial probe. It is also a STED probe in both fixed and live cells and due to its very high photostability, 3D-STED images below 40 nm resolutions can be collected.

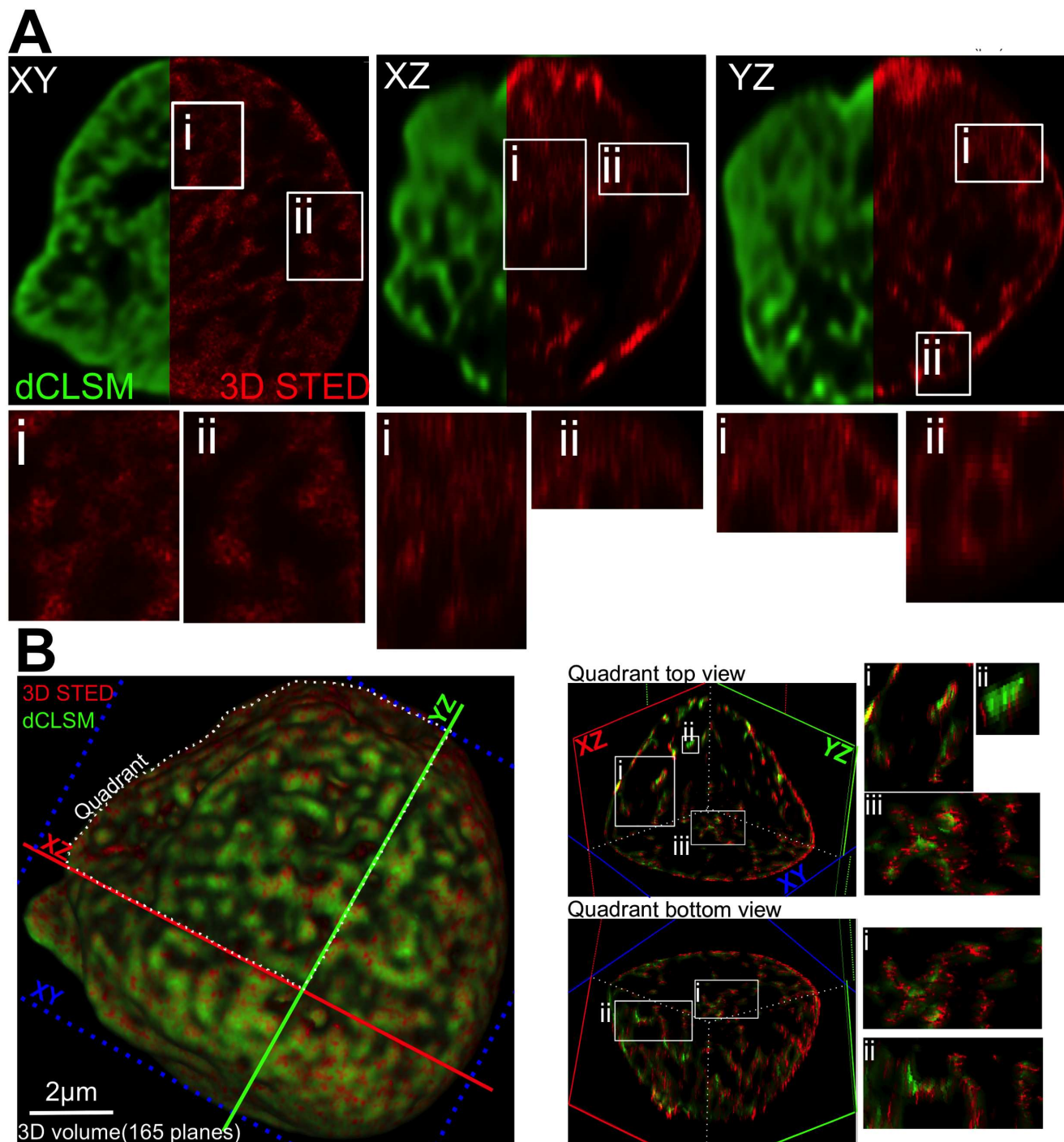


**Figure 7:** A. 3D HyVolution (dCLSM) and 3D-STED individual plane comparison for XY, XZ, YZ planes, the white squared insets are magnified next to the images (i, ii). B. 3D-STED Super resolved reconstruction of the whole nucleus volume (full 3D volume, out of 156 planes), where each single plane was imaged at the highest X, Y and Z STED resolution (3D STED). Merged dCLSM and STED reconstructed 3D surface rendered images in green and red colour respectively. Planes dividing the volume in quadrants (XY, XZ, and YZ). White squared insets reveal the super resolved nuclear structure in the Z plane (i, ii) and in the XY plane (iii) as seen in the view from the top, and in the XY (i) plane, and Z plane (ii) as seen in the view from the bottom

This complex can be synthesized on a multigram scale and images subcellular structures without laborious attachment to targeting moieties or the use of tagged/FP fusion protein constructs.

Given that this probe displays a large Stokes Shift and near infrared emission it offers great potential for multi-colour STED imaging.<sup>32</sup> Furthermore, since derivatives that

target other cellular structures are already known,<sup>36</sup> this class of compounds offers excellent potential as versatile probes for SRM and related techniques. Studies to address these issues are underway and will form the basis of future reports.

## ASSOCIATED CONTENT

### SUPPORTING INFORMATION

Experimental details, additional images and videos

### AUTHOR INFORMATION

#### Corresponding Authors

\* Email: patrina.pellett@ge.com , jorge.bernardino-de-laserna@stfc.ac.uk , james.thomas@sheffield.ac.uk

### ACKNOWLEDGMENT

(We are grateful to the EPSRC/University of Sheffield Doctoral Fellowship (MG). SS is grateful for a PhD studentship through the University of Sheffield funded 2022 Futures scheme Imagine: Imaging Life. HKS is thankful for a scholarship from KRG. JBS and EG are grateful for support from a Marie Curie Career Integration Grant "NanodynacTCELLvation" PCIG13-GA-2013-618914

### REFERENCES

- (1) Michalet, X.; Pinaud, F. F.; Bentolila, L. A.; Tsay, J. M.; Doose, S.; Li, J. J.; Sundaresan, G.; Wu, A. M.; Gambhir, S. S.; Weiss, S. *Science* **2005**, *307* (5709), 538.
- (2) Ben N G Giepmans; Adams, S. R.; Ellisman, M. H.; Tsien, R. Y. *Science* **2006**, *312* (5771), 217.
- (3) Baker, M. *Nature* **2011**, *478* (7367), 137.
- (4) Weissleder, R.; Pittet, M. J. *Nature* **2008**, *452* (7187), 580.
- (5) Thomas, J. A. *Chem Soc Rev* **2015**, *44*, 4494.
- (6) Zhu, H.; Fan, J.; Du, J.; Peng, X. *Acc. Chem. Res.* **2016**, *49* (10), 2115.
- (7) Gray, N. *Nat Cell Biol* **2009**, *11* (S1), S8.
- (8) Stender, A. S.; Marchuk, K.; Liu, C.; Sander, S.; Meyer, M. W.; Smith, E. A.; Neupane, B.; Wang, G.; Li, J.; Cheng, J.-X.; Huang, B.; Fang, N. *Chem. Rev.* **2013**, *113* (4), 2469.
- (9) Bates, M.; Huang, B.; Dempsey, G. T.; Zhuang, X. *Science* **2007**, *317* (5845), 1749.
- (10) Heilemann, M.; van de Linde, S.; Schüttelpe, M.; Kasper, R.; Seefeldt, B.; Mukherjee, A.; Tinnefeld, P.; Sauer, M. *Angew. Chem. Int. Ed.* **2008**, *47* (33), 6172.
- (11) Hell, S. W. *Science* **2007**, *316* (5828), 1153.
- (12) Clausen, M. P.; Galiani, S.; Serna, J. B. de L.; Fritzsche, M.; Chojnacki, J.; Gehmlich, K.; Lagerholm, B. C.; Eggeling, C. *NanoBiomed Imaging* **2014**, *1* (1), 1.
- (13) Gustafsson, M. *Proc. Natl. Acad. Sci. U.S.A.* **2005**, *102* (37), 13081.
- (14) Blom, H.; Widengren, J. *Chem. Rev.* **2017**.
- (15) Lukinavičius, G.; Reymond, L.; Umezawa, K.; Sallin, O.; D'Este, E.; Göttfert, F.; Ta, H.; Hell, S. W.; Urano, Y.; Johnsson, K. *J. Am. Chem. Soc.* **2016**, *138* (30), 9365.
- (16) Gustafsson, M. G. L.; Shao, L.; Carlton, P. M.; Wang, C. J. R.; Golubovskaya, I. N.; Cande, W. Z.; Agard, D. A.; Sedat, J. W. *Biophys. J.* **2008**, *94* (12), 4957.
- (17) Keene, F. R.; Smith, J. A.; Collins, J. G. *Coord. Chem. Rev.* **2009**, *253* (15-16), 2021.
- (18) McKinley, A. W.; Lincoln, P.; Tuite, E. M. *Coord. Chem. Rev.* **2011**, *255* (21-22), 2676.
- (19) Gill, M. R.; Thomas, J. A. *Chem Soc Rev* **2012**, *41* (8), 3179.
- (20) Baggaley, E.; Weinstein, J. A.; Williams, J. A. *Coord. Chem. Rev.* **2012**, *256* (15), 1762.
- (21) Lo, K. K.-W. *Acc. Chem. Res.* **2015**, *48* (12), 2985.
- (22) Rajput, C.; Rutkaite, R.; Swanson, L.; Haq, I.; Thomas, J. A. *Chem. Eur. J.* **2006**, *12* (17), 4611.
- (23) Lutterman, D. A.; Chouai, A.; Liu, Y.; Sun, Y.; Stewart, C. D.; Dunbar, K. R.; Turro, C. *J. Am. Chem. Soc.* **2008**, *130* (4), 1163.
- (24) Gill, M. R.; Garcia-Lara, J.; Foster, S. J.; Smythe, C.; Battaglia, G.; Thomas, J. A. *Nat Chem* **2009**, *1* (8), 662.
- (25) Baggaley, E.; Gill, M. R.; Green, N. H.; Turton, D.; Sazanovich, I. V.; Botchway, S. W.; Smythe, C.; Haycock, J. W.; Weinstein, J. A.; Thomas, J. A. *Angew. Chem. Int. Ed.* **2014**, *53* (13), 3367.
- (26) Wragg, A.; Gill, M. R.; Hill, C. J.; Su, X.; Meijer, A. J. H. M.; Smythe, C.; Thomas, J. A. *Chem. Commun.* **2014**, *50*, 14494.
- (27) Byrne, A.; Burke, C. S.; Keyes, T. E. *Chem. Sci.* **2016**, *7* (10), 6551.
- (28) Saini, A. K.; Sharma, V.; Mathur, P.; Shaikh, M. M. *Sci. Rep.* **2016**, *6*, 1.
- (29) Murphy, M. P. *BBA-Bioenergetics* **2008**, *1777* (7-8), 1028.
- (30) Serafim, T. L.; Oliveira, P. J.; Sardao, V. A.; Perkins, E.; Parke, D.; Holy, J. *Cancer Chemother Pharmacol* **2007**, *61* (6), 1007.
- (31) Pellett, P. A.; Sun, X.; Gould, T. J.; Rothman, J. E.; Xu, M.-Q.; Corrêa, I. R.; Bewersdorf, J. *Biomed. Opt. Express* **2011**, *2* (8), 2364.
- (32) Sednev, M. V.; Belov, V. N.; Hell, S. W. *Methods Appl Fluoresc* **2017**, *3* (4), 1.
- (33) Willig, K. I.; Harke, B.; Medda, R.; Hell, S. W. *Nat Meth* **2007**, *4* (11), 915.
- (34) Osseforth, C.; Moffitt, J. R.; Schermelleh, L.; Michaelis, J. *Opt Express* **2014**, *22* (6), 7028.
- (35) Wildanger, D.; Medda, R.; Kastrup, L.; Hell, S. W. *J Microsc* **2009**, *236* (1), 35.
- (36) Gill, M. R.; Cecchin, D.; Walker, M. G.; Mulla, R. S.; Battaglia, G.; Smythe, C.; Thomas, J. A. *Chem. Sci.* **2013**, *4* (12), 4512.

SYNOPSIS TOC (Word Style “SN\_Synopsis\_TOC”). If you are submitting your paper to a journal that requires a synopsis graphic and/or synopsis paragraph, see the Instructions for Authors on the journal’s homepage for a description of what needs to be provided and for the size requirements of the artwork.

